Study of COD and turbidity removal from real oxide-CMP wastewater by iron electrocoagulation and the evaluation of specific energy consumption

Wei-Lung Chou [a],*, Chih-Ta Wang [b], Shih-Yu Chang [a]

[a] *Department of Safety, Health and Environmental Engineering, Hungkuang University, No. 34 Chung-Chie Road, Sha-Lu, Taichung 433, Taiwan*
[b] *Department of Safety Health and Environmental Engineering, Chung Hwa University of Medical Technology, Tainan Hsien 717, Taiwan*

ABSTRACT

This study explores the feasibility of reducing COD and turbidity from real oxide chemical mechanical polishing (oxide-CMP) wastewater. Based on the dynamic characteristics of batch electrocoagulation, three operating stages (lag, reactive, and stabilizing) are proposed to identify the relationships among the zeta potential of the silica particles, solution turbidity, and the corresponding mean particle size. Experiment results show that the silica particles were destabilized and settled at the critical electrolysis time, which was estimated to be about 12 min under an applied voltage of 20 V and a supporting electrolyte of 200 mg/L. The corresponding turbidity removal occurred mostly during the reactive stage. The process variables, including applied voltage and electrolyte concentration, were investigated in terms of COD removal efficiency and turbidity removal. In addition, the effects of applied voltage and supporting electrolyte on COD removal efficiency and specific energy consumption were evaluated. Under the optimum balance, satisfactory removal efficiency and relatively low energy consumption were obtained. The optimum electrolyte concentration and applied voltage were found to be 200 mg/L NaCl and 20 V, respectively. Under the optimum conditions, COD and turbidity decreased by more than 90% and 98% in real oxide-CMP wastewater, respectively.

1. Introduction

The semiconductor industry is one of the most important manufacturing industries in Taiwan. The chemical mechanical polishing (CMP) process represents an important operation and widely adopted in the wafer fabrication processes. The CMP process has emerged as a solution for surface global planarization, and has been widely used in fabricating microchips for integrated circuits (IC), semiconductors, hard disks, optical glass, and micro-electromechanical systems [1]. The chemical–mechanical synergistic effect on CMP processes is important for a wide range of potential applications [2,3]. The process is mainly used for "polishing" the device side of a semiconductor wafer via the mechanical downward force of a slurry abrasive in association with the chemical oxidation of the wafer surface. Due to this slurry that is used in the CMP process, a large amount of ultra pure water is required to wash out abrasives that have adhered to the surface of wafers [4]. According to a previous report [4], CMP processes may account for 40% of water consumption in the semiconductor industry, and the quantity of wastewater generated is thus proportional to the water used in the CMP process [5]. Moreover, the resulting wastewater

streams need proper treatment to comply with local regulations before being discharged into surface water systems, and thus methods to treat it more efficiently are topics of interest to the industry.

Real CMP wastewater has the nature of high alkalinity, total solids content, and turbidity (in the range of 100–300 NTU). In addition, untreated real CMP wastewaters are mostly rich in organic matter consumed by the bacteria and algae normally present in healthy water sources, leading to an increased concentration of these microorganisms. The inorganic and organic contaminants in the CMP effluent derive mostly from the CMP slurry [6], and the content of insoluble inorganic contaminants depends on the type of slurry used. Inorganic contaminants in CMP wastewater may include suspended solids of SiO_2, Al_2O_3, or CeO_2 that typically have concentrations in the range of 50–500 mg/L. Organic contaminants may include metal complexing agents, surfactants, stabilizers, and rheology control agents [7]. Chemical oxygen demand (COD) is a measure of the amount of oxygen used in the chemical oxidation of inorganic and organic matter contained in wastewater. It is also considered as an indicator of the degree of pollution in the effluent, and of the potential environmental impact of the discharge of wastewater. Currently, chemical coagulation or membrane separation processes are used widely to treat CMP wastewater in the semiconductor industry [8]. CMP wastewater possesses highly negative surface charges that repel adjacent particles when they are submerged in alkaline solutions. Due to these wastewater char-

* Corresponding author. Tel.: +886 4 26318652x4005; fax: +886 4 26319175.
E-mail address: wlchou@sunrise.hk.edu.tw (W.-L. Chou).

acteristics, removing such nano-scale particles by conventional chemical coagulation is not ideal. In order to resolve these problems, electrochemical treatment techniques have attracted a lot of attention because of their versatility and environmental compatibility. Using electrons, which are a "clean reagent" [9], as the main reagent, an electrochemical treatment method has been proposed to treat wastewater containing dispersed fine particles without chemical addition [10–14]. Belongia et al. [15] first investigated the particle removal phenomena of synthetic alumina and silica solution using electrodecantation and electrocoagulation. Electrocoagulation is an electrochemical method of treating polluted water whereby sacrificial anodes dissolve due to an applied voltage, producing active coagulant precursors. Sacrificial anodes of iron and aluminum are commonly used to continuously supply metallic ions as the source of coagulation. These electrochemically generated metallic ions can hydrolyze near the anode to form a series of metallic hydroxides capable of destabilizing dispersed particles. The electrocoagulation process utilizes the effect of charge neutralization/surface complexation/adsorption onto the in situ formed metal hydroxides generated from the oxidation of corrodible anode materials. Pollutants are then removed by sedimentation and become the slurry [16]. Electrocoagulation is a water treatment technology that has been applied to treat various wastewaters, including potable water [17,18], urban wastewater [19], heavy metal laden wastewater [20–22], restaurant wastewater [23], colored water [24], dyeing wastewater [25,26], wastewater containing phosphate [27,28], mechanical cutting oil [29], fluoride [30], and arsenic [31]. Previous researchers have mostly studied the removal characteristics and CMP wastewater quality before and after electrocoagulation treatment [10,11]. To extend our early investigation of treating synthetic oxide-CMP wastewater and to discuss silica particle settling characteristics [32], in this study, electrocoagulation was employed to treat real oxide-CMP wastewater from a large semiconductor plant in central Taiwan in an attempt to remove the suspended silica particles, reduce the wastewater turbidity, and decrease the COD concentration.

The dynamic characteristics (e.g., zeta potential and mean particle size) of suspended silica particles in the real oxide-CMP wastewater during electrocoagulation were monitored. These characteristics were investigated to determine the optimum treatment conditions and to explain the dynamic nature of batch electrocoagulation by considering three stages: lag, reactive, and stabilizing. Parameters, such as applied voltage and supporting electrolyte concentration, both of which govern the removal performance, were also investigated in terms of COD removal efficiency and turbidity. In addition, an effective process must also be economically feasible with regard to its electrical energy consumption, and practically applicable to environmental problems. Electrical energy consumption is itself a very important economic parameter in the electrocoagulation process, and so the effect of two operational parameters (applied voltage and supporting electrolyte) on the specific energy consumption (SEC) under the optimum conditions was also evaluated in this study.

2. Experimental

2.1. Properties of real oxide-CMP wastewater

Real oxide-CMP wastewater was obtained from a dynamic random access memory (DRAM) manufacturing unit in Central Taiwan Science Park, Taichung, Taiwan. The oxide-CMP wastewater had a diluted milky color, indicative of the presence of the fine suspended oxide particles [10]. Table 1 shows the chemical and physical properties of the real oxide-CMP wastewater used in this study. The real oxide-CMP wastewater had a high total

Table 1
Water properties of real oxide-CMP wastewater.

Parameter	Real oxide-CMP wastewater
pH	8–9
Conductivity (μs/cm)	100–200
Turbidity (NTU)	200–300
Mean particle size (nm)	85–95
Zeta potential (mV)	−28 to −35
COD (mg/L)	300–600
TOC (mg/L)	3–5
SS (mg/L)	10–20
TS (mg/L)	4000–5000

solids content of 4000–5000 mg/L, a suspended solids (SS) concentration of 10–20 mg/L, turbidity in the range of 200–300 NTU, a TOC of 3–5 mg/L, a COD of 400–600 mg/L, a conductivity of 100–to 200 μs/cm, a pH of between 8 and 9, a zeta potential of between −28 mV and −35 mV, and a mean particle size between 85 nm and 95 nm. All samples were measured in duplicate to ensure data reproducibility, and an additional measurement was carried out if necessary.

2.2. Equipment

A diagram of the experimental apparatus and the electrode assembly used for electrocoagulation is shown schematically in Fig. 1. The electrolytic cell was a 1-L pyrex glass reactor equipped with a water jacket and a magnetic stirrer. The temperature of the electrolytic cell was controlled by continuously circulating water through the water jacket from a refrigerated circulating bath (Scilab, BL-720, Taiwan). A magnetic stirrer (Suntex, SH-301, Taiwan) was employed in the reactor to maintain adequate mixing of the CMP wastewater during the electrocoagulation process. From our previous studies on synthetic oxide-CMP wastewater, we know that the Fe/Al electrode pair is the optimum choice of the four electrode pair combinations [32]. Therefore, cast iron (Fe) and aluminum (Al) plates (8 cm × 4 cm × 0.5 cm) were used as the anode/cathode pair. The electrode pair was dipped in the CMP wastewater to a depth of 4.5 cm, with the electrodes approximately 2 cm apart. The effective area of the electrode pair was 18 cm^2. Electrical voltage was provided by a manually controllable DC power supply (Fann-chern, GC50-20D, Taiwan) operating in the constant voltage mode (range: 0–50 V). Characterization of the CMP wastewater, such as pH (Y.S.I, pH10, USA), conductivity (EUTEOH, cyberscan 510, Singapore), turbidity (in terms of Nephelometric turbidity unit, NTU; HACH, 2100P,
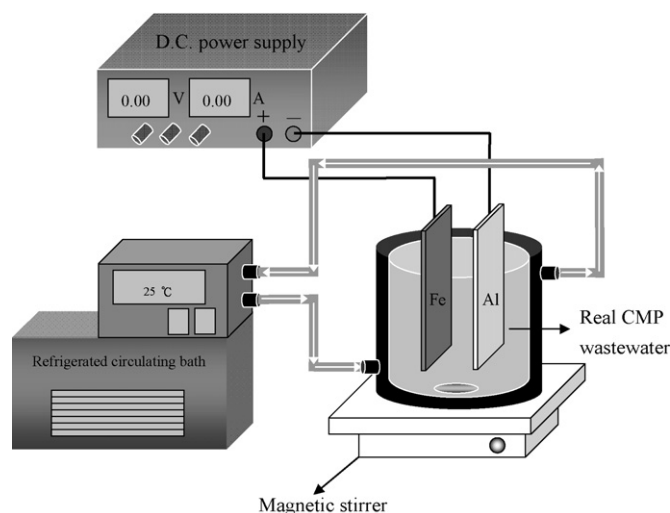

Fig. 1. Schematic diagram of the experimental setup.

USA), TOC (Systematic, Model 1030W, USA), and total solids (TS), were determined using ROC EPA standard methods [33]. A Malvern zeta potential and size analyzer (Malvern Instruments, Zetasizer Nano Series, UK) was used to determine the zeta potential and particle size distribution of the suspended silica particles in the CMP wastewater.

2.3. Chemicals and reagents

The pH of the solution was adjusted by adding either dilute sulfuric acid (H_2SO_4) or sodium hydroxide (NaOH). Stock H_2SO_4 and NaOH solutions of 0.1 M were freshly prepared by dissolving reagent grade H_2SO_4 (Scharlau, Chemie, SA, SPAIN) and NaOH (Sigma–Aldrich, Germany) in deionized water, respectively. The conductivity of solutions was adjusted to different values by the addition of NaCl (Tedia Company, USA). The COD concentration of samples was measured using a HACH Model DR2800 spectrophotometer (HACH Company, USA), and the analysis was conducted by the procedures described in Standard Methods [34]. The calculation of COD removal efficiency after the electrocoagulation treatment was performed using this formula:

$$R\ (\%) = \frac{COD_0 V_0 - COD_t V_t}{COD_0 V_0} \times 100 \tag{1}$$

where COD_0 is the initial concentration in mg/L, COD_t is the concentration value at time t in mg/L, V_0 is the initial volume of the treated wastewater in liters, and V_t is the volume of the treated wastewater at time t in liters.

2.4. Method

Before each experiment, the electrodes were abraded with sand paper to remove scale, then dipped in 3 M H_2SO_4 to a depth of 6 cm for 30 min, and finally cleaned with successive rinses of water. During each test run, 0.5 L of CMP wastewater was placed in the reactor. The magnetic stirrer was turned on and set at 300 rpm. A steady temperature of 25 °C was maintained for all test runs. The stirrer speed was found to be sufficient to provide good mixing in the electrolytic cell, and yet was not strong enough to break up the flocs formed during the treatment process. A fixed amount of between 100 mg/L and 300 mg/L (NaCl) was added to the CMP wastewater to increase the wastewater conductivity and thus facilitate the electrocoagulation treatment. The DC power supply was turned on with constant voltages of 10 V, 20 V, and 30 V, respectively. An electrocoagulation test run lasted no more than 60 min in all experiments. At the end of electrocoagulation, all samples were allowed to settle for 5 h in a 20 mL pyrex glass column. The turbidity of the CMP wastewater after electrocoagulation treatment was determined using a turbidity meter, while the COD of samples were analyzed using a HACH Model DR/2800 spectrophotometer.

3. Results and discussion

3.1. Characterization of real oxide-CMP wastewater

The concept of surface potential (i.e., zeta potential) is a valuable practical parameter for coagulation and the resultant separation from the aqueous solution, providing a direct indicator of solution stability. Fig. 2 indicates the zeta potential of the suspended silica particles and the corresponding particle size as a function of the solution pH. The solution pH of real oxide-CMP wastewater was adjusted and maintained by the addition of the required amount of NaOH or H_2SO_4. As can be seen in Fig. 2, an increase in pH led to a greater degree of negative zeta potential and a decrease in the corresponding particle size. For example, by increasing the pH of the solution from about 2 to 10, the zeta potential changed from
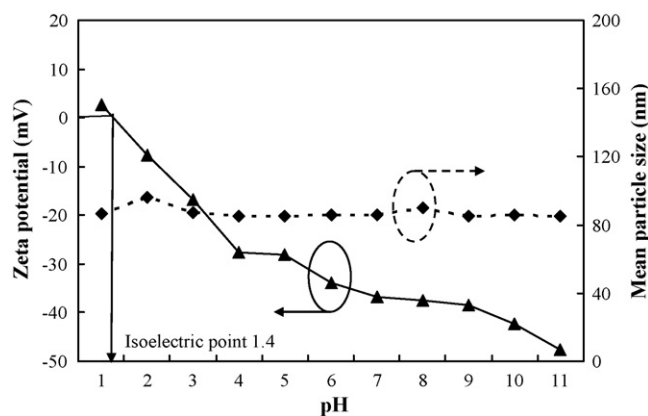

Fig. 2. Effect of solution pH on the zeta-potential and mean particle size of real oxide-CMP wastewater.

−7.6 mV to −42.3 mV and the mean particle size decreased from 96.1 nm to 80.8 nm. This may be attributed to the pH increase in the real oxide-CMP wastewater causing the silica particles to adsorb more OH^- ions on the particle surface and creating $Si–O^-$ on the surface, thus resulting in greater negative zeta potential. Electrostatic repulsion between the particles of the electric double layers with greater negative potential drives suspended particles apart, leading to particle stability and reducing the particle size. Accordingly, the relatively smaller mean particle size associated with the suspended silica of real oxide-CMP wastewater can be attributed to its relatively large negative zeta potential. Furthermore, the isoelectric point at which charge reversal is observed for the suspended silica of real oxide-CMP wastewater was about 1.4, corresponding to a mean particle size of approximately 97 nm.

3.2. Effect of applied voltage

Among the various operating parameters in all the electrochemical processes, the applied voltage is an important factor which strongly influences the performance of electrocoagulation [35]. The effects of applied voltage on the COD removal efficiency and the turbidity of real wastewater were studied at 10 V, 20 V, and 30 V levels. In order to evaluate these effects, a series of experiments was conducted with 250 NTU initial turbidity, 571 mg/L initial COD concentration, 200 mg/L NaCl concentration, 8.5 initial pH, and a 300 rpm agitation speed. Fig. 3 indicates the effect of applied voltage on the COD removal efficiency for various durations of electrolysis. As the time of electrolysis increases, comparable
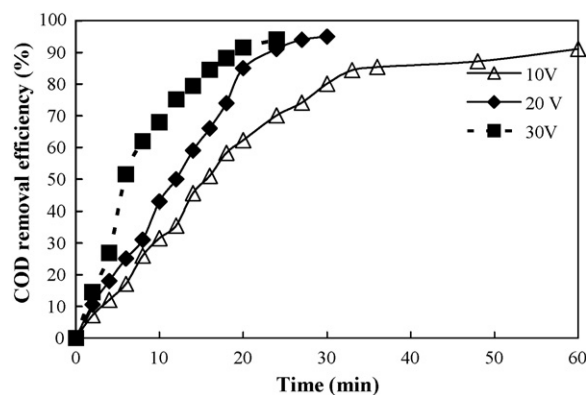

Fig. 3. Effect of applied voltage on the COD removal efficiency during electrocoagulation with Fe/Al electrode pair, 571 mg/L initial COD, 250 NTU initial turbidity, 200 mg/L NaCl, 300 rpm agitation speed.
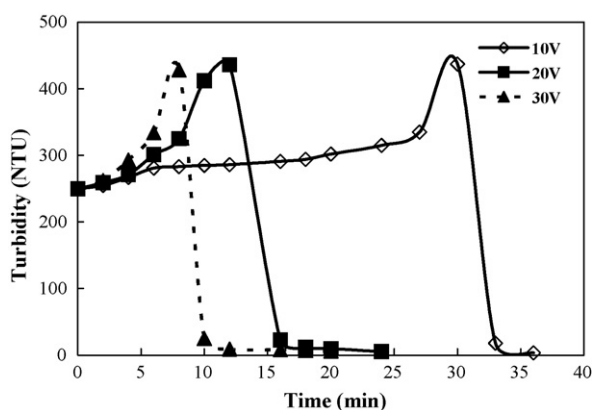
Fig. 4. Effect of applied voltage on the turbidity during electrocoagulation with Fe/Al electrode pair, 571 mg/L initial COD, 250 NTU initial turbidity, 200 mg/L NaCl, 300 rpm agitation speed.

5120 nm, and 247 nm to 5160 nm when the treatment time reached 10 min, 16 min, and 33 min for 30 V, 20 V, and 10 V, respectively. These observations imply that the suspended silica particles in real oxide-CMP wastewater were destabilized to settle at the mean particle size that rapidly increased in this period. The corresponding turbidity removal mostly occurred during this period. In order to study and explain this phenomenon, the dynamic characteristics of suspended silica particles during electrocoagulation are investigated in the subsequent section.

3.3. Effect of the concentration of the supporting electrolyte

Solution conductivity affects the cell voltage, current efficiency, and consumption of electrical energy in electrolytic cells. Therefore, the electrical conductivity of the solution is an important parameter for saving electric energy in an electrochemical cell. More energy is required for overcoming a high ohmic resistance between an anode and a cathode when the electrical conductivity of the solution is low. In this study, the original conductivity of the real oxide-CMP wastewater from a semiconductor plant was in the range of 100–200 μs/cm, as shown in Table 1. This solution is not conductive enough for electrocoagulation treatment. The most common method used to overcome this problem is to add a small amount of supporting electrolyte, which increases the conductivity of the solution and thus reduces the energy consumption during electrocoagulation [37,38]. In this study, sodium chloride (NaCl) was used as the supporting electrolyte for increasing the conductivity of the real oxide-CMP wastewater. When investigating the supporting electrolyte's influence on the COD removal efficiency, the value of the applied voltage was 20 V, the electrode pair was the Fe/Al combination, the initial COD concentration was 571 mg/L, and the temperature was 25 °C. Fig. 5 shows the effect of the NaCl concentration on the COD removal efficiency for various durations of electrolysis. With increasing electrocoagulation time, appreciable increases in the COD removal efficiency were observed regardless of the supporting electrolyte concentration. As the concentration of the supporting electrolyte increased, the COD removal efficiency of the real oxide-CMP wastewater also increased. The COD removal efficiency reached 78%, 85%, and 92% after 20 min of electrolysis

improvements in the COD removal efficiency were observed for all applied voltages. It can be seen that the COD removal efficiency reached 62.3%, 85.3%, and 91.5% after 20 min of electrolysis for 10 V, 20 V, and 30 V, respectively. As the applied voltage increased, so did the COD removal efficiency. This was probably because the organic compounds present in the real oxide-CMP wastewater that reacted with iron ions (Fe (II) or Fe (III)) to form insoluble compounds were mostly removed. The required treatment time to reach over 90% COD removal efficiency was 20 min, 24 min, and 60 min for 30 V, 20 V, and 10 V, respectively. Fig. 4 illustrates the effect of various applied voltages on the turbidity of real oxide-CMP wastewater for various durations of electrolysis where the sludge was allowed to settle for over 5 h. As can be seen in Fig. 4, the final turbidity removal of wastewater reached over 90% in less than 10 min and 16 min of electrocoagulation for 30 V and 20 V, respectively. As the applied voltage increased, the length of each electrocoagulation process decreased. Due to a sufficient voltage through the solution, the metal ions generated by the dissolution of the sacrificial electrode were hydrolyzed to form a series of metallic hydroxide species. These species neutralized the electrostatic charges on the dispersed particles to reduce the electrostatic interparticle repulsion enough for the van der Waal's attraction to predominate, thus facilitating agglomeration [36]. However, it took a longer time (about 33 min) to reach over 90% turbidity removal for an applied voltage of 10 V. This is because the applied voltage of 10 V was unable to completely destabilize the suspended oxide particles in the solution. Therefore, both 20 V and 30 V are suitable operating applied voltages for this electrocoagulation experiment, requiring treatment times of less than 16 min. The influence of the applied voltage, regardless of voltage value, in the beginning period on the turbidity of real oxide-CMP wastewater was interesting. Fig. 4 indicates that the turbidity of the real oxide-CMP wastewater increased gradually in the first 8 min, 12 min, and 30 min for 30 V, 20 V, and 10 V, respectively. This could be explained by insufficient coagulant dissolving from the iron anode at the beginning of electrocoagulation, effectively reducing the double layer of the suspended particles to destabilize them, resulting in inadequately large particles to settle and thus enhanced turbidity. Table 2 summarizes the dynamic variation of particle size of the suspended silica and the corresponding turbidity in real oxide-CMP wastewater during electrocoagulation. As can be seen in Table 2, the turbidity of the real oxide-CMP wastewater increased gradually in the beginning period and decreased abruptly from 479 NTU to 18 NTU, 436 NTU to 24 NTU, and 428 NTU to 25 NTU after 10 min, 16 min, and 33 min of treatment time for 30 V, 20 V, and 10 V, respectively. The corresponding mean particle size increased dramatically from 189 nm to 6255 nm, 172 nm to

Table 2
Effect of various applied voltages on real wastewater turbidity and particle size for various durations of electrolysis.

EC time (min)	Turbidity (NTU)	Particle size (nm)
10 V		
0	250	93.
6	281	95
12	286	98
18	294	100
24	311	108
27	314	112
30	**479**	**247**
33	**18**	**5160**
20 V		
0	250	94
4	271	97
8	325	106
12	**436**	**172**
16	**24**	**5120**
30 V		
0	250	92
2	262	95
4	293	100
6	334	117
8	**428**	**189**
10	**25**	**6255**

The significance of bold values in Table 2 is to emphasize an abrupt decrease in the turbidity of solution and a significant increase in silica particle size of solution.
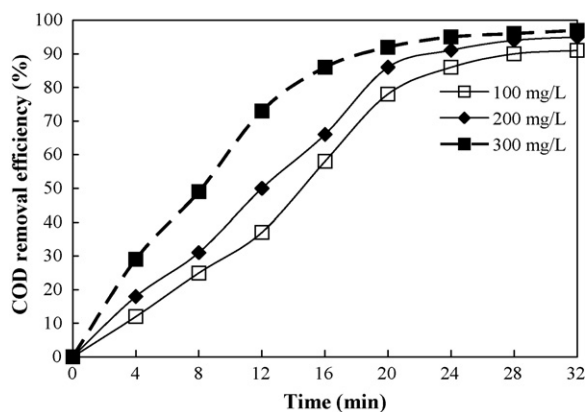
Fig. 5. Effect of supporting electrolyte concentration on the COD removal efficiency during electrocoagulation with Fe/Al electrode pair, 571 mg/L initial COD, 250 NTU initial turbidity, 20 V applied voltage, 300 rpm agitation speed.

for 100 mg/L, 200 mg/L, and 300 mg/L, respectively. It can be also seen that the treatment time to reach 90% COD removal efficiency was around 20 min, 24 min, and 28 min for 300 mg/L, 200 mg/L, and 100 mg/L, respectively.

Fig. 6 indicates the effect of various supporting electrolyte concentrations on the turbidity variation of real oxide-CMP wastewater for various durations of electrolysis. As can be seen in Fig. 6, the excellent final turbidity of oxide-CMP reached over 90% in less than 20 min of electrolysis for NaCl concentrations of 200 mg/L and 300 mg/L. When the concentration of the supporting electrolyte (NaCl) was increased from 100 mg/L to 200 mg/L, the required treatment time to reach 90% turbidity removal was improved greatly from 36 min to 16 min. However, no significant improvement in the required treatment time to reach 90% turbidity removal was observed when the concentration of the supporting electrolyte was increased from 200 mg/L to 300 mg/L. This shows that an excess amount of NaCl in the solution is detrimental to removal of turbidity.

Fig. 6 also shows that the turbidity of the real oxide-CMP wastewater increased gradually in the first 12 min, 12 min, and 24 min for 300 mg/L, 200 mg/L, and 100 mg/L, respectively. This is also shown in Fig. 4, which may be attributed to inadequate coagulant generated from the anode at the beginning of electrolysis, reducing the double layer of the silica particles to destabilize them, causing insufficient large particles to settle and thus increase turbidity. Consequently, in terms of the COD and turbidity removal
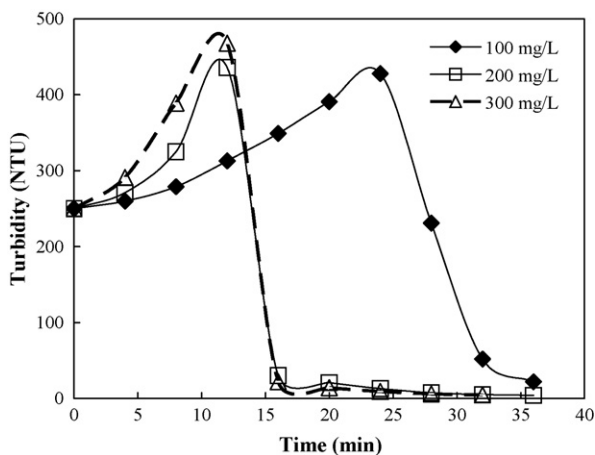
shown in Figs. 5 and 6, respectively, the effect of NaCl addition was significant. This was probably because the Cl^- anions can destroy the passivation layer and increase the anodic dissolution rate of metal, either by the incorporation of Cl^- into the oxide film or by the participation of Cl^- in the metal dissolution reaction [39]. In addition, the increase of the chloride ion concentration in the solution can reduce the overpotential in the anodic oxidation of chloride ions, resulting in a higher current efficiency [40,41]. The problem of electrode passivation is a serious drawback in the present applications of electrocoagulation, so destroying the passivation layer and hence enhancing the dissolution rate of Fe or Al is thus crucial. The de-passivation effect was more significant when more Cl^- anions were added to the solution. Therefore, the problem of electrode passivation was partially solved and the performance of the electrocoagulation process was increased when NaCl was used as the electrolyte.

3.4. Dynamic characteristics of silica particles during the electrocoagulation process

Many coagulation mechanisms of suspended particles, including surface charge neutralization, double layer compression, adsorption and bridging, have been proposed that depend on the chemical and physical properties of the aqueous solution, pollutant, and coagulant [42,43]. As previously discussed, colloid particles were maintained in stable suspension by the electrostatic repulsion between particles. Zeta potential is regarded as an effective measurement of the charge of a particle while it migrates to the solution, thus providing an indicator of solution stability. Generally, the electrocoagulation process is inherently dynamic, with ferrous ions entering the system, being hydrolyzed with suspended particles, and then removed from the system. To investigate of the dynamic characteristics of silica particles during electrocoagulation, the zeta potential of the oxide particles and the corresponding turbidity were measured during the treatment period. The changes during the course of electrocoagulation for the applied voltage of 20 V and the supporting electrolyte of 200 mg/L are shown in Fig. 7. It can be obviously seen from this figure that there were three stages, defined as lag, reactive, and stabilizing, during the electrocoagulation process [32]. Fig. 7 shows that the zeta potential of silica particles remained relatively steady in a range of −40 mV to −38 mV for the first 12 min—a response that is considered as the lag stage. An increase in turbidity was observed during this stage, which might be ascribed to the aggregated particle size in this period being not big enough to settle. As time progressed and
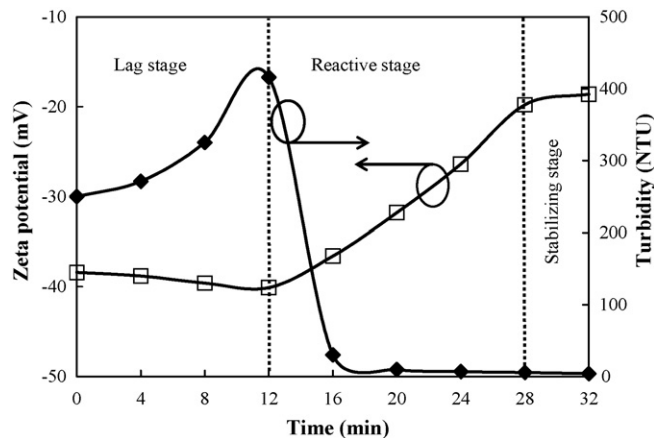

Fig. 6. Effect of supporting electrolyte concentration on the turbidity during electrocoagulation with Fe/Al electrode pair, 571 mg/L initial COD, 250 NTU initial turbidity, 20 V applied voltage, 300 rpm agitation speed.

Fig. 7. Effect of wastewater zeta potential and turbidity during electrocoagulation with the Fe/Al electrode pair, 571 mg/L initial COD, 250 NTU initial turbidity, 20 V applied voltage, 200 mg/L NaCl, 300 rpm agitation speed.

dissolved coagulants from the iron electrode increased, a period was reached where there was an abrupt increase in the zeta potential (i.e., a small degree of negative zeta potential). The majority (~98%) of turbidity removal occurred during this reactive stage. Therefore, the beginning of the reactive stage might be defined as the period where a rapid decrease in turbidity starts. As the system moved into the stabilizing stage, the rate of turbidity removal continued to decrease until it approached zero, while the corresponding zeta potential reached a plateau in the range of −20 mV to −18 mV after 28 min of electrolysis. The stable increase in the zeta potential after a short steady period reveals that electrocoagulation appeared as a double layer compression [44]. As time progressed and the amount of coagulants (i.e., iron cations) produced at the anode increased, these suppressed the electric double layer suspended silica particles and destabilized these particles, thus promoting the aggregation of the suspended silica particles. As can be seen in Fig. 7, at the beginning of the reactive stage, the turbidity started to decrease rapidly after 12 min of electrolysis. At this time, the zeta potential increased (i.e., a small degree of negative zeta potential), which resulted in the aggregation of the silica particles and the generation of bigger particles. The corresponding mean particle size increased dramatically from 172 nm to 5120 nm as the treatment time increased from 12 min to 16 min for the applied voltage of 20 V and the supporting electrolyte of 200 mg/L, as shown in Table 2. These observations imply that the suspended silica particles were destabilized to settle at the critical electrolysis time, which was estimated to be 12 min for the applied voltage of 20 V and the supporting electrolyte of 200 mg/L. The corresponding turbidity removal mostly occurred during this period (i.e., the reactive stage).

3.5. Evaluation of specific energy consumption

Ultimately, it is not the highest removal efficiency, but rather the electric energy consumption required to achieve the desired degree of treatment that will determine the feasibility of a proposed treatment approach. Consequently, it is critical to evaluate the electrical energy consumption of wastewater treatment to decide whether electrocoagulation is economically as well as technically viable for the COD removal of real oxide-CMP wastewater. COD values are related to the total concentration of organics in the solutions. Once the required voltages and the corresponding currents were obtained from the electrocoagulation tests, it was possible to estimate the amount of energy required. We considered the initial and final concentrations of COD in real oxide-CMP wastewater at different times. The specific energy consumption was then calculated as a function of 1 kg COD removal of real oxide-CMP wastewater during electrocoagulation in kW h/kg with a constant applied voltage using the following equation [45]:

$$SEC = \frac{U \int I \, dt}{(COD_0 \times V_0 - COD_t \times V_t) \times 3.6}$$

$$= \frac{U \times I_{avg} \times \Delta t}{(COD_0 \times V_0 - COD_t \times V_t) \times 3.6} \quad (2)$$

where U, I_{avg}, and Δt are the applied voltage (V), average current (A), and electrolysis time (sec), respectively. In addition, COD_0 is the initial concentration of COD in mg/L, COD_t is the concentration value of compounds at time (t) in mg/L, V_0 is the initial volume of the treated wastewater in liters, and V_t is the volume of the treated wastewater at time t in liters. In order to investigate the optimum balance with reasonable COD removal efficiency and relatively low energy consumption, the applied voltage and the amount of the supporting electrolyte during electrocoagulation are optimized in the following section.
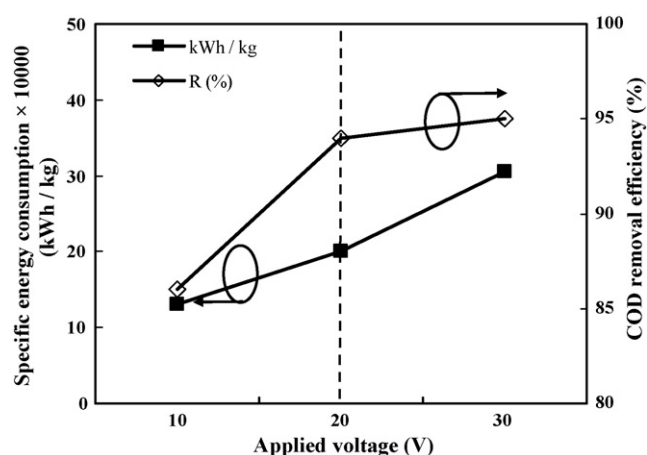

Fig. 8. Effect of applied voltage on the specific energy consumption and COD removal efficiency after 20 min of electrolysis with Fe/Al electrode pair, 571 mg/L initial COD, 250 NTU initial turbidity, 200 mg/L NaCl, 300 rpm agitation speed.

3.5.1. Effect of applied voltage on specific energy consumption and COD removal efficiency

In order to evaluate the effect of applied voltage on the specific energy consumption and COD removal efficiency, a series of electrocoagulation experiments were carried out on real oxide-CMP wastewater after 20 min electrolysis. The initial COD concentration was set at 571 mg/L, a fixed amount of 200 mg/L supporting electrolyte was added to the real oxide-CMP wastewater, the agitation speed was 300 rpm, and the electrode distance was 2 cm. The real oxide-CMP wastewater with applied voltages in the range of 10–30 V was treated in terms of the specific energy consumption and COD removal efficiency by iron electrocoagulation, as shown in Fig. 8. It can be seen that the specific energy consumption increased by increasing the applied voltage, which increased the COD removal efficiency. When the applied voltage was increased from 10 V to 20 V, the COD removal efficiency was raised appreciable from 62.3% to 77.3%, whereas the corresponding specific energy consumption increased only slightly. However, when the applied voltage was increased from 20 V to 30 V, the COD removal efficiency increased only slightly from 77.3% to 82.5%, whereas the corresponding specific energy consumption increased significantly. When considering both specific energy consumption and COD removal efficiency simultaneously, the applied voltage of 20 V provides the optimum balance for the present electrocoagulation, with a reasonable COD removal efficiency and relatively low specific energy consumption.

3.5.2. Effect of supporting electrolyte on specific energy consumption and COD removal efficiency

To investigate the effect of the supporting electrolyte on the specific energy consumption and COD removal efficiency, a number of experiments were performed after 20 min of electrolysis with 571 mg/L initial COD concentration, 20 V applied voltage, 2.5 initial pH, 300 rpm agitation speed, and 2 cm electrode distance. The concentration of supporting electrolyte was adjusted to the desired level by adding a suitable amount of NaCl to the real oxide-CMP wastewater. Fig. 9 indicates the effect of various supporting electrolyte concentrations on the performance of COD removal efficiency and specific energy consumption during the electrocoagulation process. It can be seen that increasing the concentration of supporting electrolyte increases the COD removal efficiency, while significantly increasing the specific energy consumption. When the concentration of the supporting electrolyte was increased from 100 mg/L to 200 mg/L, the COD removal efficiency increased from 78% to 86%, while the corresponding specific
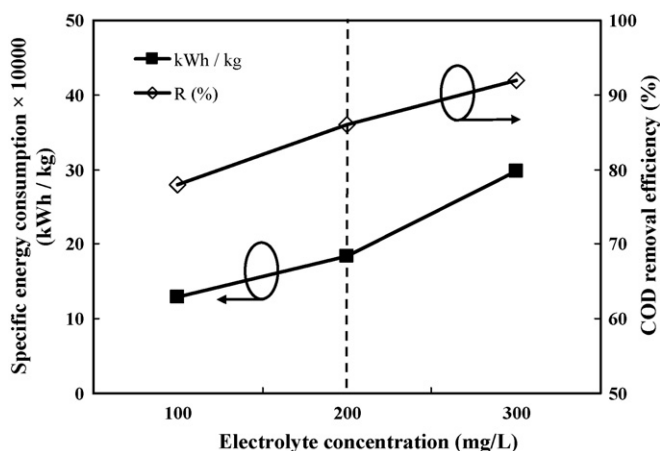
Fig. 9. Effect of supporting electrolyte concentration on the specific energy consumption and COD removal efficiency after 20 min of electrolysis with Fe/Al electrode pair, 571 mg/L initial COD, 250 NTU initial turbidity, 20 V applied voltage, 300 rpm agitation speed.

energy consumption increased slightly from 1.29×10^{-3} kW h/kg to 1.84×10^{-3} kW h/kg. However, when the concentration of the supporting electrolyte increased from 200 mg/L to 300 mg/L, the COD removal efficiency increased slightly from 86% to 92%, while the corresponding specific energy consumption increased from 1.84×10^{-3} kW h/kg to 2.98×10^{-3} kW h/kg. Accordingly, when considering both the specific energy consumption and the COD removal efficiency, 200 mg/L NaCl provides the optimum balance with desirable COD removal efficiency and relatively low specific energy consumption.

4. Conclusion

The results of this study show the applicability of electrocoagulation in removing turbidity and COD from real oxide-CMP wastewater from a large semiconductor plant in central Taiwan. In order to investigate the dynamic characteristics of silica particles from real oxide-CMP wastewater during electrocoagulation, three operating stages (lag, reactive, and stabilizing) were proposed to identify the relationships among the zeta potential of the silica particles, the turbidity of the suspended solution, and the corresponding mean particle size of the suspended silica. Experimental results show that the suspended silica particles were destabilized to settle at the critical electrolysis time, which was estimated to be 12 min of electrolysis for an applied voltage of 20 V and a supporting electrolyte of 200 mg/L. The corresponding turbidity removal mostly (98%) occurred during this period (i.e., the reactive stage). Furthermore, the corresponding mean particle size varied from 172 nm to 5120 nm as the treatment time progressed from 12 min to 16 min, which also occurred during the reactive stage. For low specific energy consumption and good COD removal efficiency, an applied voltage of 20 V was found be the optimum overall within the test range of between 10 V and 30 V with reasonable COD removal efficiency and relatively low specific energy consumption. 200 mg/L NaCl provides the optimum balance with desirable COD removal efficiency and relatively low specific energy consumption.

References

[1] F.B. Kaufman, D.B. Thompson, R.E. Broadie, M.A. Jaso, W.L. Guthrie, D.J. Pearson, M.B. Small, Chemical mechanical polishing for fabricating patterned W metal features as chip interconnects, J. Electrochem. Soc. 138 (1991) 3460–3465.
[2] J. Xu, J.B. Luo, X.C. Lu, C.H. Zhang, G.S. Pan, Progress in material removal mechanisms of surface polishing with ultra precision, Chin. Sci. Bull. 49 (2004) 1687–1693.
[3] Y.G. Wang, Y.W. Zhao, W. An, J. Wang, Modeling the effects of cohesive energy for single particle on the material removal in chemical mechanical polishing at atomic scale, Appl. Surf. Sci. 253 (2007) 9137–9141.
[4] G. Corlett, Targeting water use for chemical mechanical polishing, Solid State Technol. 43 (2000) 201–206.
[5] G.C.C. Yang, CMP wastewater management using the concepts of design for environment, Environ. Prog. 21 (2002) 57–62.
[6] J.H. Golden, J.E. Carrubba, Chemistry of CMP wastewater, Semicond. Fabtech. 13 (2001) 123–126.
[7] J.H. Golden, R. Small, L. Pagan, C. Shang, S. Ragavan, Evaluating and treating CMP wastewater, Semicond. Int. 23 (2000) 92–103.
[8] S. Browne, V. Krygier, J. O'Sullivan, E.L. Sandstrom, Treating wastewater from CMP using ultrafiltration, MICRO 17 (1999) 5–14.
[9] L.J.J. Janssen, L. Koene, J. Chem, The role of electrochemistry and electrochemical technology in environmental protection, Chem. Eng. 85 (2002) 127–136.
[10] C.L. Lai, S.H. Lin, Electrocoagulation of chemical mechanical polishing (CMP) wastewater from semiconductor fabrication, Chem. Eng. J. 95 (2003) 205–211.
[11] C.L. Lai, S.H. Lin, Treatment of chemical mechanical polishing wastewater by electrocoagulation: system performances and sludge settling characteristics, Chemosphere 54 (2004) 235–242.
[12] W. Den, C. Huang, Electrocoagulation for removal of silica nano-particles from chemical–mechanical–planarization wastewater, Colloids Surf. A 254 (2005) 81–89.
[13] C.L. Lai, K.S. Lin, Sludge conditioning characteristics of copper chemical mechanical polishing wastewaters treated by electrocoagulation, J. Hazard. Mater. B 136 (2006) 183–187.
[14] N. Drouiche, N. Ghaffour, H. Lunici, M. Mameri, Electrocoagulation of chemical mechanical polishing wastewater, Desalination 214 (2007) 31–37.
[15] B.M. Belongia, P.D. Haworth, J.C. Baygents, S. Raghvan, Treatment of alumina and silica chemical polishing waste by electro-decantation and electrocoagulation, J. Electrochem. Soc. 146 (1999) 4124–4130.
[16] M.Y.A. Mollah, P. Morkovsky, J.A.G. Gomes, M. Kesmez, J. Parga, D.L. Cocke, Fundamentals, present and future perspectives of electrocoagulation, J. Hazard. Mater. B 114 (2004) 199–210.
[17] E.A. Vik, D.A. Carlson, A.S. Eikum, E.T. Gjessing, Electrocoagulation of potable water, Water Res. 18 (1984) 1355–1360.
[18] P.K. Holt, G.W. Barton, M. Wark, C.A. Mitchell, A quantitative comparison between chemical dosing and electrocoagulation, Colloids Surf. A 211 (2002) 233–248.
[19] M.T. Pouet, A. Grasmick, Urban wastewater treatment by electrocoagulation and flotation, Water Sci. Technol. 31 (1995) 275–283.
[20] D. Mills, A new process for electrocoagulation, J. Am. Water Works Assoc. 92 (2000) 35–43.
[21] A.K. Golder, A.N. Samanta, S. Ray, Removal of Cr^{3+} by electrocoagulation with multiple electrodes: bipolar and monopolar configurations, J. Hazard. Mater. 141 (2007) 653–661.
[22] I. Heidmann, W. Calmano, Removal of Zn(II), Cu(II), Ni(II), Ag(I) and Cr(VI) present in aqueous solutions by aluminum electrocoagulation, J. Hazard. Mater. 152 (2008) 934–941.
[23] X. Chen, G. Chen, L.Y. Po, Separation of pollutants from restaurant wastewater by electrocoagulation, Sep. Purif. Technol. 19 (2000) 65–76.
[24] J.Q. Jiang, N. Graham, C. Andre, H.K. Geoff, N. Brandon, Laboratory study of electro-coagulation–flotation for water treatment, Water Res. 36 (2002) 4064–4078.
[25] N. Daneshvar, A. Oladegaragoze, N. Djafarzadeh, Decolorization of basic dye solutions by electrocoagulation: an investigation of the effect of operational parameters, J. Hazard. Mater. B 84 (2006) 116–122.
[26] İ.A. Şengil, M. Özacar, The decolorization of C.I. reactive black 5 in aqueous solution by electrocoagulation using sacrificial iron electrodes, J. Hazard. Mater. 161 (2009) 1369–1376.
[27] Ş. İrdemez, N. Demircioğlu, Y.Ş. Yildiz, Z. Bingül, The effects of current density and phosphate concentration on phosphate removal from wastewater by electrocoagulation using aluminum and iron plate electrodes, Sep. Purif. Technol. 52 (2006) 218–223.
[28] Ş. İrdemez, Y.Ş. Yildiz, V. Tosunoğlu, Optimization of phosphate removal from wastewater by electrocoagulation with aluminum plate electrodes, Sep. Purif. Technol. 52 (2006) 394–401.
[29] K. Bensadok, S. Benammar, F. Lapicque, G. Nezzal, Electrocoagulation of cutting oil emulsions using aluminum plate electrodes, J. Hazard. Mater. 152 (2008) 423–430.
[30] N. Mameri, H. Lounici, D. Belhocine, H. Grib, D.L. Piron, Y. Yahiat, Defluoridation of Sahara water by small plant electrocoagulation using bipolar aluminum electrodes, Sep. Purif. Technol. 24 (2001) 113–119.
[31] J.R. Parga, D.L. Cocke, J.L. Valenzuela, J.A. Gomes, M. Kesmez, G. Irwin, H. Moreno, M. Weir, Arsenic removal via electrocoagulation from heavy metal contaminated groundwater in La Comarca Lagunera Mexico, J. Hazard. Mater. B 124 (2005) 247–254.

[32] C.T. Wang, W.L. Chou, L.S. Chen, S.Y. Chang, Silica particles settling characteristics and removal performances of oxide chemical mechanical polishing wastewater treated by electrocoagulation technology, J. Hazard. Mater. 161 (2009) 344–350.

[33] ROC Environmental Protection Administration (EPA), Standard Environmental Methods for Water Quality, http://www.niea.gov.tw/niea/WATER/, 2007 (in Chinese).

[34] American Public Health Association (APHA), Standard Methods for the Examination of Water and Wastewater, 17th ed., APHA, Washington, DC, 1992.

[35] D. Pletcher, F.C. Walsh, Industrial Electrochemistry, 2nd ed., Chapman and Hall, London, UK, 1990.

[36] M.Y.A. Mollah, R. Schennach, J. Parga, D.L. Cocke, Electrocoagulation (EC)—science and applications, J. Hazard. Mater. B 84 (2001) 29–41.

[37] S.H. Lin, C.C. Chang, Treatment of landfill leachate by combined electro-fenton oxidation and sequencing batch reactor method, Water Res. 34 (2000) 4243–4249.

[38] C.T. Wang, Decolorization of congo red with three-dimensional flow-by packed-bed electrodes, J. Environ. Sci. Heal. A 38 (2003) 399–413.

[39] W.J. Lee, S.I. Pyun, Effects of hydroxide ion addition on anodic dissolution of pure aluminum in chloride ion-containing solution, Electrochim. Acta 44 (1999) 4041–4049.

[40] J.S. Do, W.C. Yeh, I.Y. Chao, Kinetics of oxidative degradation of formaldehyde with electrogenerated hypochlorite ion, Ind. Eng. Chem. Res. 36 (1997) 349–356.

[41] K. Vijayaraghavan, T.K. Ramanujam, N. Balasubramanian, In situ hypochlorous acid generation for the treatment of distillery spent wash, Ind. Eng. Chem. Res. 38 (1999) 2264–2267.

[42] W.J. Eilbeck, G. Mattock, Chemical Process in Waste Water Treatment, Ellis Horwood Limited, Chichester, 1987.

[43] D.N. Thomas, S.J. Judd, N. Fawcett, Flocculation modeling: a review, Water Res. 33 (1999) 1579–1592.

[44] L.D. Benefield, F.C. Judkins, B.L. Weand, Process Chemistry for Water and Wastewater Treatment, Prentice-Hall, Englewood Cliffs, NJ, 1982.

[45] N. Daneshvar, A.R. Khataee, A.R. Amani Ghadim, M.H. Rasoulifard, Decolorization of C.I. Acid Yellow 23 solution by electrocoagulation process: investigation of operational parameters and evaluation of specific electrical energy consumption (SEEC), J. Hazard. Mater. 148 (2007) 566–572.